STUDY ABOUT BOIL IN ACTUAL RIVER

ATSUHIRO YOROZUYA
Public Works Research Institute, Tsukuba, Japan, yorozuya@pwri.go.jp

AHMAD ALI GUL
Former National Graduate Institute for Policy Studies, Tokyo, Japan

TSUYOSHI HOSHINO
Graduate school of Engineering, Hokkaido University, Sapporo, Japan, hoshino@eng.hokudai.ac.jp

SHOJI OKADA
National Institute of Technology, Kochi College, Nangoku, Japan, okada@ce.kochi-ct.ac.jp

ABSTRACT

The present study discusses about the boil phenomena. The target flow field is the one observed in the Brahmaputra river, whose flow field has the area of 1,000m×200m, flow depth is about 9m, and discharge is about 3,500m^3/s. The Reynolds number at the occurrence of the boil is 1.4×10^7. Three different method are compared; such as observed flow field by ADCP, modified observed-flow by the mass-consistent method, and the numerically simulated flow by the URANS implementing the observed geometry and flow properties. The URANS model successfully simulated the boil phenomena. Regarding the flow structure, three different characteristics are recognized, such as a) high upward velocity generates at the stoss side, b) longitudinal velocity affected by the a), and c) the down-ward velocity generated at the top of the crest as a paired type flow with the a). Relating to the occurrence of the boil, the higher bed shear stress also recognized by the ADCP observation and the simulated one.

Keywords: ADCP, bedform, boil, mass-consistent model, and URANS

1. INTRODUCTION

Boils or kolk-boils are one of the coherent structures in turbulence flow and they are classified as ‘boil of first kind’ by Nakagawa and Nezu (1993). The phenomena in actual rivers plays important role to the sediment transport rate, in particularly to concentration of fine sediment. Kinoshita (1984) discussed the flow field during flooding in actual river with aerial photo, and reported that high concentration of the suspended sediment relates to the boil. Nezu (1993) conducted the experimental study and examined the effects of the boil phenomena to the suspended-sediment concentration.

Recently, thanks to a high specification computer as well as a recent technique of the numerical simulation, understanding of the turbulent flow has improved. For example, a numerical model; such as DNS or LES, successfully simulates the coherent structure in turbulent flow. A Unsteady Reynold-Averaged Navier-Stokes (URANS) model, which requires less computation resources, can partly simulate the separation vortex; e.g., Kimura and Hosoda (2004). In addition to that, the relationship between the turbulence flow and behavior of fine sediment was discussed. For example, Sekine (2007) simulated one of the bursting phenomena in turbulence; e.g., a sweep motion, by LES. And he showed that the seep motion is dominate to the equilibrium sediment concentration at the reference level. This study verified the one by Ashida, and Michiue (1970).

On the other hand, thanks to the recent technologies of the acoustic type; e.g., Acoustic Doppler Current Profiler (ADCP), the measurement of the sediment transport rate in the actual river have been reported. One of examples are the bed load discharge measurement (Rennie 2002, Yorozuya et al., 2010, and Koseki et al.,2017), and suspended sediment (Kitsuda et al., 2002). With implementing those technique, Okada et al. (2016) reported the observed results of the flow and sediment transport rate in the Brahmaputra river in Bangladesh. In addition to that, Gul et al. (2018) observed the boil of first kind by ADCP. One of the major contributions of them is reporting the observed results of the boil in very high Reynolds number, the flow field, the bed load discharge, and the suspended sediment concentration. With onsite measurement of the water sampling, he reported that the size distribution is larger and sediment concentration is considerably higher than other non-boil area. This result indicated the important role of the boil phenomena to the suspended sediment.

In order to deepen the discussion about the boil phenomena reported by Gul et al. (2018), the present study discuss about the flow field and the shear stress at the vicinity of the boil area. Regarding to the flow field, three data sets are compared; such as 1) the observed data by ADCP, 2) the observed data modified by the mass-consistent method, and 3) flow field simulated by 3-D numerical simulation with the URANS model. Regarding to the shear stress, two data sets are compared; such as 1) the shear stress observed by ADCP's bedload velocity, and 3) the one simulated by the URANS model.

2. METHODOLOGY

2.1 Flow and sediment transport rate measurement by ADCP

The measurement was conducted with RiverRay ADCP operating at 600 kHz manufactured by Teledyne RD instruments and a Starfire WDGPS mounted on a tethered boat. The tethered boat was towed by a manned control-boat. In order to obtain the bed material, the dredge-type sampler was used. The suspended sediment concentration and its size distribution were obtained by a water sampler. The measurement site is Brahmaputra river near the city of Bahadurabad in Bangladesh. The river section around this point is about 10 km including several bars and channel, and about 60,000 m^3/s of discharge was observed. Sediment size is about 0.2 mm and mostly this river section is suspended-sediment dominated. An area of interest of the current study located at a left-most channel of this section and it has the size of 200 m × 1,000m as shown in Figure 1.

Implementing the water-depth data obtained by ADCP, the river-bed elevation, as shown in Figure 1, is defined as a relative scale, whose zero is a water surface. The water surface slope in this area is about 1/14,000 estimated by locally installed gauges. In order to obtain the bathymetry as shown in Figure 1, two types of boat operation were conducted. One is setting up the boat at the upstream end of this domain (at 1000m in Figure1), and letting the boat move with relative zero-velocity along stream flow. The other is moving back to the upstream end while observing data. Those two operations were repeated until the boat pass was dense enough to create the bathymetry. Inverse Distance Weighted method (IDW) was implemented to create the 2-D grid type data sets. 11 transects of observation was conducted for this measurement in 3.5 hours. Other measured flow properties, such as velocity in three-dimensional manner and echo intensities, were distributed to create the 3-D grid system by IDW. The bottom track values are treated as same as the bathymetry.

As Figure 1 shows, there are some angulation in this area, which could be a micro-scale bed form. There are two lines in this figure. The Line 1 is the pass where the boil does not take place, while the line 2 is the pass where the boil takes place. The Point A is the location where the boil take place.

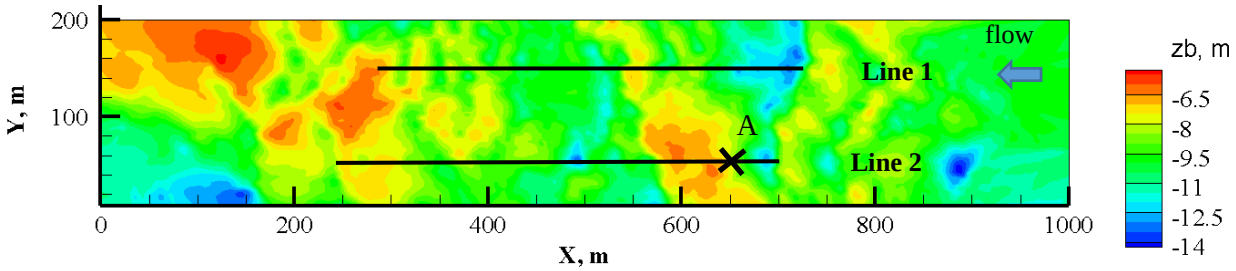

Figure 1 Bathymetry obtained by ADCP measurement (Z = 0 is water surface)

2.2 Mass-consistent method

One of the characteristics of ADCP is the profiling technique. The technique is able to obtain a profiling data set in few second with using the four-beams spreading 20 degree. The assumption of the technique is a homogeneity of the flow field. In the case where the homogeneity cannot be guaranty, the velocity in vertical direction should be carefully taken care. For taking care, the mass-consistent method (Sherman, 1978) is implemented.

$$E(u,v,w,\lambda) = \int_V \left[\alpha_1^2(u-u^0)^2 + \alpha_1^2(v-v^0)^2 + \alpha_2^2(w-w^0)^2 + \lambda\left(\frac{\partial u}{\partial x}+\frac{\partial v}{\partial y}+\frac{\partial w}{\partial z}\right)\right] dxdydz \quad (1)$$

where u, v, and w are adjusted velocity vector in the x, y, and z direction. u^0, v^0, w^0 are corresponding observed values. λ is Lagrange multiplier. α_1 and α_2 are Gaussian precision moduli. In order to minimize the *E*, a first derivative with respected to u, v, w, and λ should be zero. Following equation can be obtained.

$$u = u^0 + \frac{1}{2\alpha_1^2}\frac{\partial \lambda}{\partial x} \tag{2}$$

$$v = v^0 + \frac{1}{2\alpha_1^2}\frac{\partial \lambda}{\partial y} \tag{3}$$

$$w = w^0 + \frac{1}{2\alpha_2^2}\frac{\partial \lambda}{\partial z} \tag{4}$$

$$\frac{\partial u}{\partial x} + \frac{\partial v}{\partial y} + \frac{\partial w}{\partial z} = 0 \tag{5}$$

Pugging equation (2), (3), and (4) in equation (5), equation (6) is derived.

$$\frac{\partial^2 \lambda}{\partial x^2} + \frac{\partial^2 \lambda}{\partial y^2} + \left(\frac{\alpha_1^2}{\alpha_2^2}\right)\frac{\partial^2 \lambda}{\partial z^2} = -2\alpha_1^2\left(\frac{\partial u^0}{\partial x} + \frac{\partial v^0}{\partial y} + \frac{\partial w^0}{\partial z}\right) \tag{6}$$

Here, α_1 and α_2 are changeable parameters with assuming the ratio of α_1 and α_2 are related to the ratio of w and u. With changing the parameters, equation (2) can be solved for λ, and u, v, w can be obtained.

Equation (6) is implemented in the numerical simulation, with other boundary condition, e.g., lateral and down-stream condition is set as velocity gradient is zero. Grid sizes are dx and dy are 2m, and number of grids in z direction is 41.

Regarding to observed results by ADCP, Δw is the one of the indicators to show the homogeneities. The authors considered that the magnitude of Δw is same as the difference between w and w^0. Therefore, present study checks those two parameters in order to justify the adjustment by the mass-consistent method.

2.3 URANS model

The present study implements URANS model developed by research group by Kimura, available in iRIC as Nays CUBE. Among them, AHK model (Ali, Hosoda & Kimura, 2007) was implemented. Riverbed evolution is not considered. The geometry as an initial condition is shown in Figure 1. The optimized model parameter of AHK is selected. Non-periodic boundary conditions in longitudinal/lateral direction are applied. Table 1 shows the other conditions.

Table 1. implemented conditions for the numerical simulation.

dt, s	dx/dy, m	Number of grid in z direction	Discharge from upstream	Water suface elevation at downsteam end, m	Roughness at bottom
0.005	2	50	3,500	0.0	0.02

In order to examine the unsteadiness of the simulated results, the firstly, the numerical simulation conducted till 120 seconds. Though simulated results have not reached to steady condition yet, it was made sure that amplitude of flow properties; water depth, damped till 0.85% after 110 seconds at where the boil took place. Therefore, present study discusses about the results at 115 seconds.

3. RESULTS

3.1 Longitudinal profile along the line 1

Figure 2, 3, and 4 shows the vertical velocity by the contour along the line, where the boil does not take place. The horizontal axis indicates the distance from downstream end, and vertical axis shows the river bed where 0 m indicates the water surface. Figure 2 is the result observed by ADCP and redistributed by IDW. Figure 3 is the one modified by Mass-consistent method, and Figure 4 is the results obtained by URANS model.

As Figure 2 indicates, there are several locations, where vertical flows take place. For example, at X = 380, 490, 560, and 630, the upward velocity can be seen. In the most of the case, they are at toss side of river bed. In particular, the one at the 380 is the strongest, and the value shows about 0.2 m/s. On the other hand, at X = 400, 510, 590, and 700, the downward velocity can be seen. They are located at the lee side of the river bed. It can be understood that those vertical velocities are results of the bed forms, since they are corelated to the shape of the river bed.

There is not much difference between Figure 2 and Figure 3. This fact indicates that correction by the mass consistent method can be negligible in such a small velocity.

As Figure 4 indicates, the flow pattern is very similar with that observed by ADCP as shown in Figure 2. These results are much clearer and higher that the results in Figure 2 and 3. They are well corresponded to the shape of the river bed, such as the stoss and lee side. Vertical velocity obtained by URANS model is about 1.5 times bigger than that obtained by ADCP.

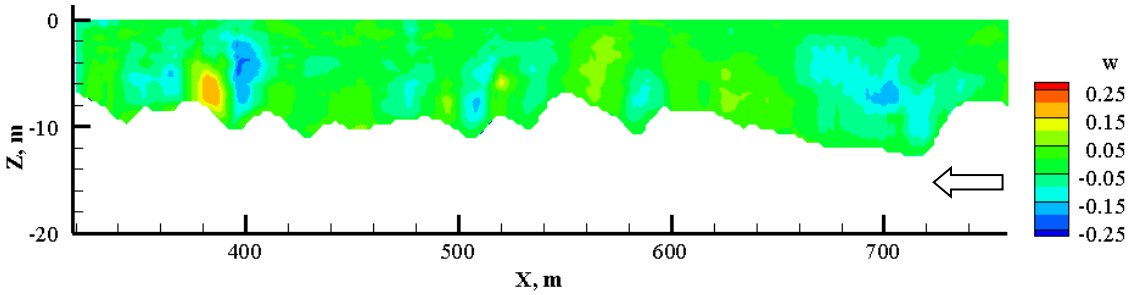

Figure 2 vertical velocity along the line 1 by ADCP-IDW similar with that of Figure 4

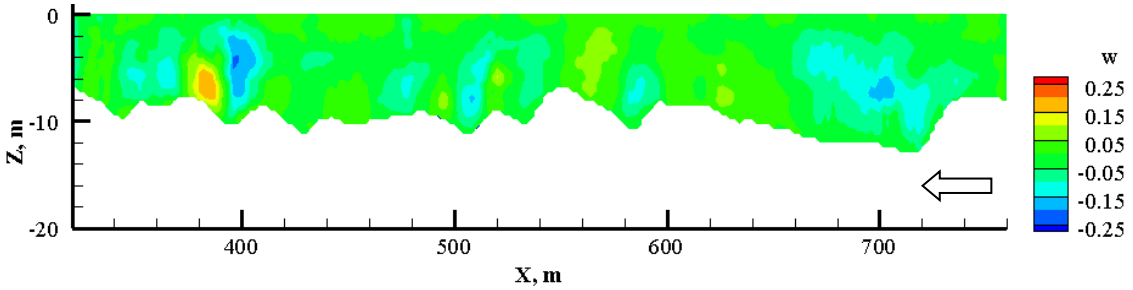

Figure 3 vertical velocity along the line 1 by ADCP-MASCON similar with that of Figure 4

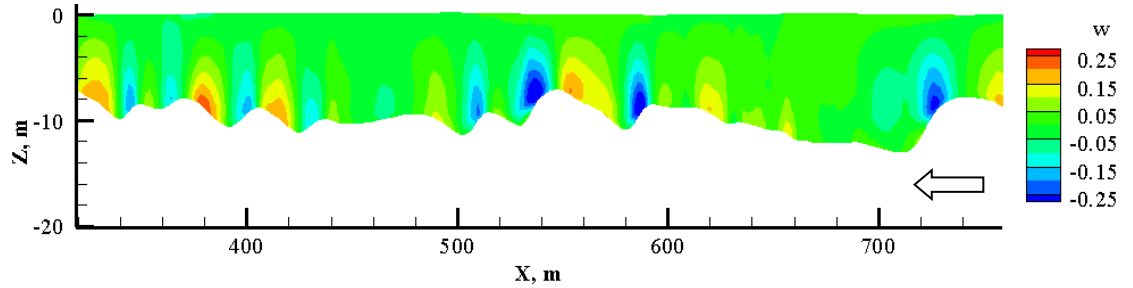

Figure4 vertical velocity along the line 1 by URANS model

Vertical velocity obtained by ADCP seems lower than that obtained by URANS model. This is reasonable trends. Actually, Hashiba et al. (2017) reported the different flow field between the first one obtained by the iRIC cube, and the second modified the first one, as if the ADCP measurement conducted. The first one is the cellular secondary current, while the second one is named as the pseudo-observed flow field. Regarding the vertical velocity, Hashiba et al. (2017) pointed out that the pseudo-observed results could be half of the cellular secondary current. Here, the present study has discussed the flow pattern around the micro-bed form, in particular the vertical velocity. The URANS model simulated this tendency very well. On the other hand, the ADCP measured vertical velocity with less value (could be half), though their observation is appropriate enough in terms of the location where the vertical velocity exist. At the same time, the Mass-consistent method is not effective enough for being similar with the one by URANS model.

3.2 Longitudinal profile along the line 2

Figure 5/6 and 7/8 show the longitudinal velocity as well as vertical velocity by the contour along the line 2, where the boil takes place. Figure 9 shows the $-\overline{w'u'}$ along line2 as well. Figure 5 and 7 are the results obtained by ADCP and modified by MASCCON. Figure 6, 8, and 9 are the results by the URANS model. They were depicted in the same manner as that of Figure 2.

As Figure 5 and 6 indicates, the longitudinal velocity correlated to the water depth. When it becomes shallower at the crest of the bed form, the velocities become faster, though there is one exception at X = 640. For example, the velocity around X = 360, 430, 600, 700 and 770 are significant. Contrary, the velocity at the section of the trough become slower, since the depth become deeper. Those reasonable trends are appropriately illustrated in the both figures, and the magnitude of the velocity are nearly equal. Unlike the vertical velocity, the longitudinal velocity by the ADCP with the Mass-consistent method is appropriately observed. In addition to that, the area of the slow velocity can be recognized in the trough, such as X = 480, 530, 550, 680, and 740. This area could be inside of the separation vortex. Therefore, it is reasonable both results show similarly, though the URANS model show less significantly. Regarding one exception, the slow u velocity can be recognized at X= 640m and Z = -4m. The authors considered this flow as the occurrence of the boil. It should be specially mentioned that the flow at t=4 does not show the trends. The boil phenomena developed as times go by. This discussion will be mainly described in the next paragraph associating with the vertical velocity.

As Figure 7 and 8 indicates, vertical velocities exist with corelating to the bed form. As explained in the Figure 2-4, the locations are strongly correlated with the bed form. Both results are well corresponded to the shape, though the URANS model is more sensitive than that by ADCP. However, in Figure 7, there is very significant exception, such as the strong upward flow around X = 650 and the down ward flow around X = 600. Regarding the flow at X = 650, the maximum velocity reached to 0.35 m/s. This vertical flow can be seen in the Figure 8, but not that high. The authors considered that the observed phenomenon at this point is boil. The slow longitudinal velocity in the Figure 5 and 6 at X= 640m and Z = -4m could be correlated with the boil, since the very fast velocity in the vertical direction induced the lower longitudinal velocity. Regarding the flow at X =600, the down ward flow exits around this area. In other location, the down-ward velocity at the lee side was well described, but not at the top of the crest. This could be one of the paired type flows with the upward flow at X = 650. It could be difficult to justify, since much has not discussed this flow pattern in the literature. However, the authors, as an observed evidence, are very sure that this down-ward flow exist at this point with some reason.

In order to discuss about the occurrence of the boil, the authors select the $-\overline{w'u'}$ as shown in Figure 9. As it shows, $-\overline{w'u'}$ is in particularly high at the location of boil. This is also one of the evidences that the coherent turbulence generated around this area.

Regarding the boil phenomenon at X = 650, Gul et al. (2018) explained it from different aspects. They saw the boil and recorded by the camera with geo tag information. In addition to that, they indicated that very high sediment concentration (SS) was observed and the size distribution of SS is larger at this point. Not only the flow field discussion with Figure 7 but also the fact recognized in the field and discussion relating to the suspended sediment concentration, the authors concluded that the phenomenon is the boil.

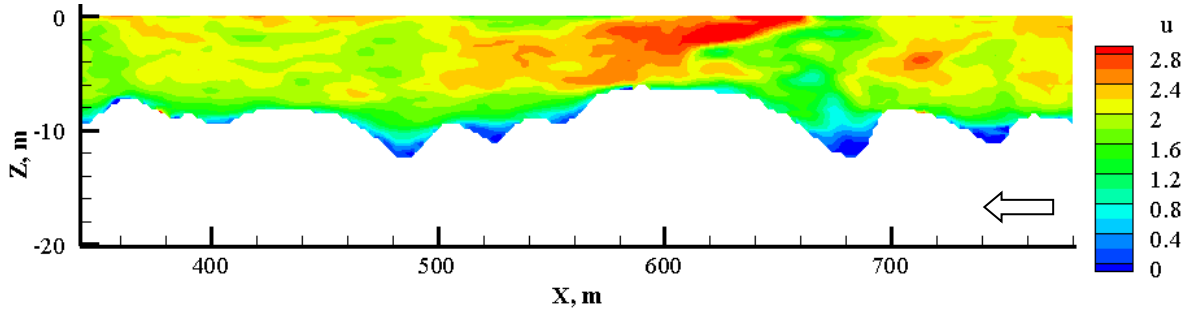

Figure 5 longitudinal velocity along the line 2 by ADCP-MASCON

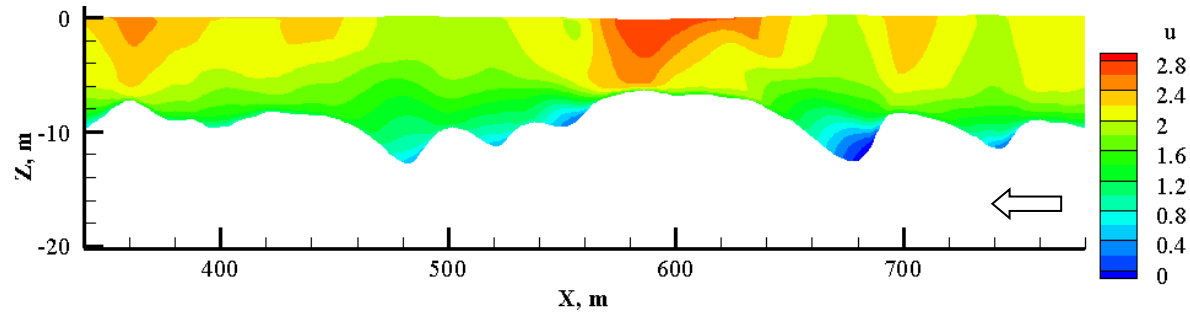

Figure 6 longitudinal velocity along the line 2 by URANS

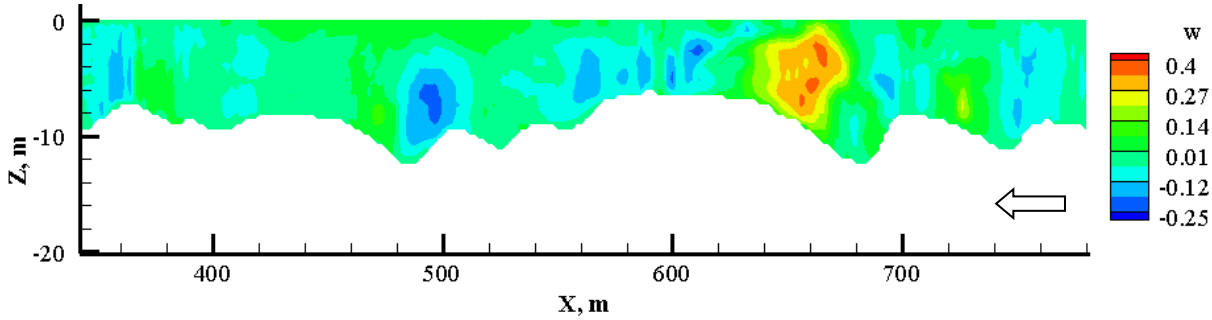

Figure 7 vertical velocity along the line 2 by ADCP-MASCON

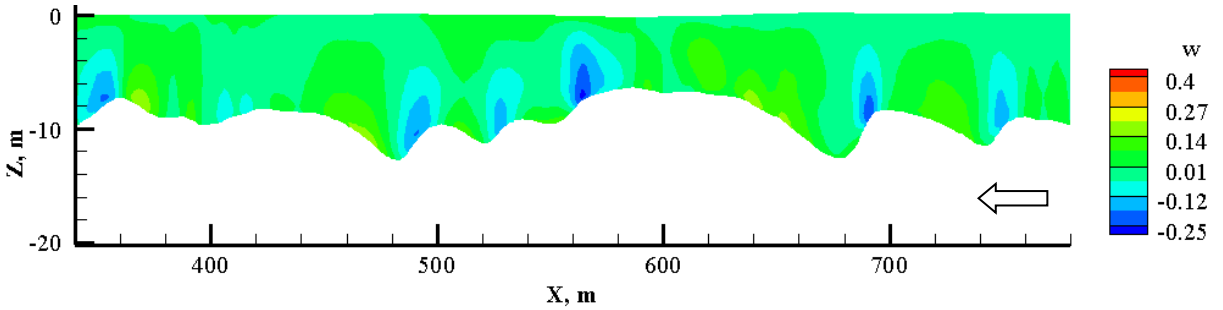

Figure 8 vertical velocity along the line 2 by URANS

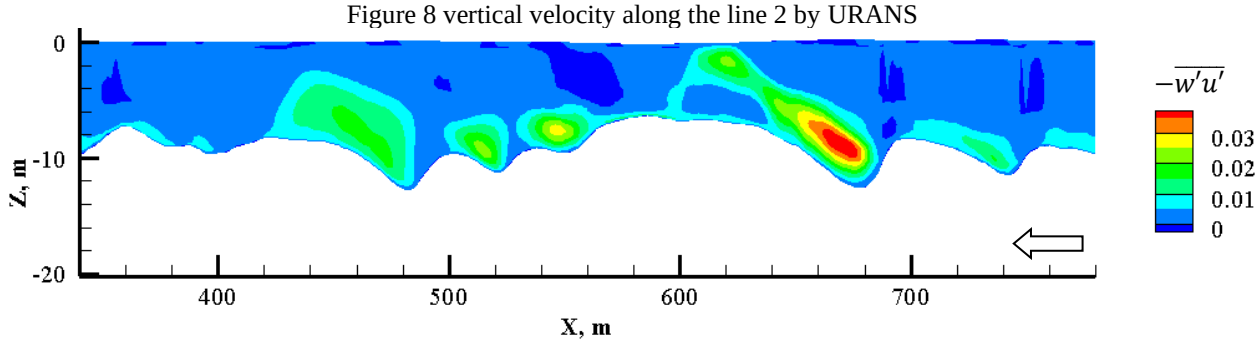

Figure 9 $-\overline{w'u'}$ along the line 2 by URANS

The authors considered that AHK model; one of the URANS models, successfully simulated the boil phenomenon as shown in Figure 6 and 9, though the upward velocity and down-ward velocity does not have that high compared with that by observed. The authors also considered that the boil phenomenon was observed by ADCP. Though ADCP cannot observes the Reynolds shear stress, still there are flow patterns associated with the boil which ADCP can observe. Based on this understanding, three significant flow field as the characteristic of the boil can be concluded, such as 1) high upward velocity generates at the stoss side; e.g., at X=640, 2) longitudinal velocity is affected by the first flow, and 3) the down-ward velocity generates at the top of the crest as a paired type flow with the first one; at X = 600.

3.3 Bed shear stress at where boil takes place

Figure 10 shows the non-dimensional shear stress; τ_*, estimated by URANS converted from the bed shear stress. The black like represents the line 2 of the Figure 1, and point A are the same with that of the Figure 1. X and Y in this figure are corresponding to all other figures. In order to obtain the τ_*, sediment diameter; such as 0.2 mm reported by Gul et al. (2018), was implemented. As seen in the figure, on the line in particular, the point at X = 690 shows the lowest value. As discussed previously, this point is inside of the trough, and it could be inside of the separated vortex as shown in Figure 6. As the point of interest moves to the downstream along the line, τ_* gradually become large, and it shows the highest value at X=640. As discussed previously, the URANS model successfully simulated the boil. Therefore, this highest value are the results of the boil. It was also specially noted that the boil does not appear in the results of t = 4 seconds as explained in the previous chapter. In the no-boil case, the highest value does not appear at t=4. There is another higher value at X=570, which is on the crest of the bed form. This higher value can be considered as the shear stress due to grain roughness. Thereafter, it gradually become small as it moves to the downstream along the line. The τ_* ratio of the one at X = 640 to X = 570 is 1.05.

Figure 11 shows the non-dimensional shear stress; τ_*, calculated by the bed load velocity; u_b, as well as the line 2 as black line and the point A. This τ_* is the one, proposed by Koseki (2017) implementing the u_b from the bottom track function and the relationship between u_b and τ_* proposed by Egashira (1997). Unlike the one of the Figure 10, which are calculated by the flow, this is the one estimated by the results of the movement of the sediment. As seen in the Figure 11, the similar trends with the Figure 10 can be seen, such as the highest value at point A, higher values on the crest, and smaller values in the trough. Regarding the highest value at point A, the location of the maximum value coincides with that of the boil. The authors have difficulty to find relationship between the shear stress and the occurrence of boil with quantitative manner. However, we are very sure that 1) the boil phenomena originated at this point somehow affects to the river bed, 2) the movement of the sediment around the riverbed are monitored by the bottom track function of ADCP as u_b, and 3) the u_b is larger than the one at the top of the crest. The τ_* ratio of the one at X = 640 to X = 570 is 1.05. In addition to that Gul et al. (2018) reported, the occurrence of the boil results the higher sediment concentration and larger particle as suspended sediment can be observed. Based on those discussion, the boil should cause the higher shear stress compared with that due to the grain roughness.

Main difference of Figure 10 and 11 are the magnitude of the value. The authors are not sure about this difference. It could be relating to the wall function, which is applied by the URANS. This discussion is out of my focus as Nays CUBE users. Therefore, the present study keeps this difference as feature discussion. On the other hand, τ_* estimated by $\sqrt{ghi}$ shows similar magnitude with that in the Figure 11. Therefore, the value of Figure 11 is more appropriate.

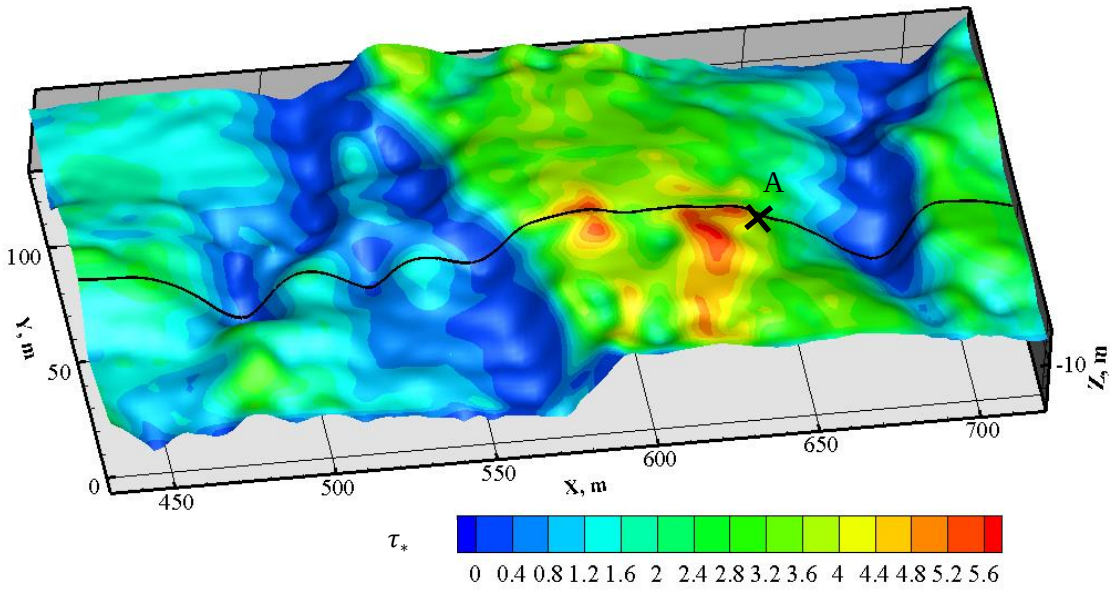

Figure 10 non-dimensional shear stress (τ* was calculated by Bed shear stress)

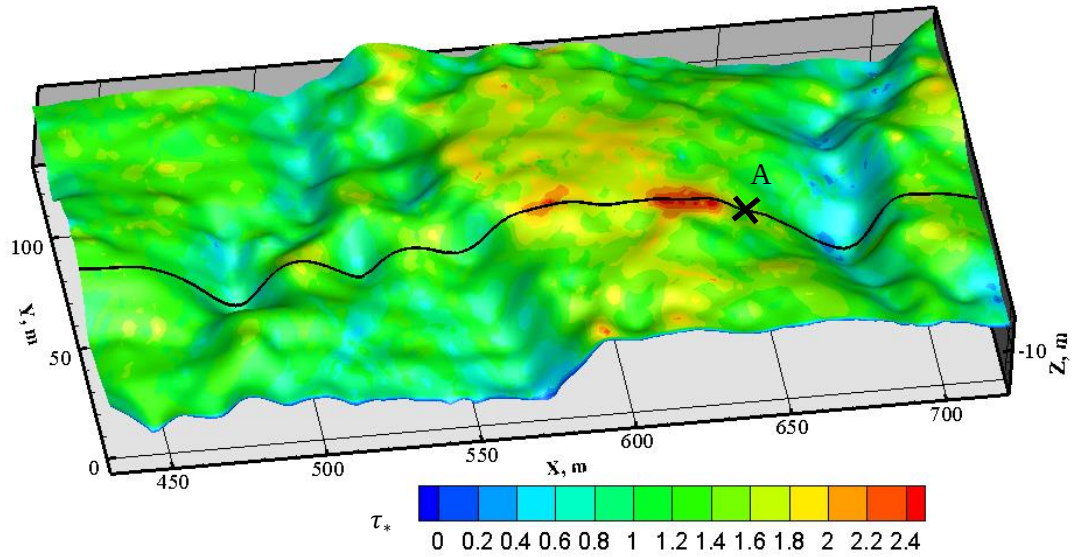

Figure 11 non-dimensional shear stress obtained converted from bedload velocity obtained by ADCP

4. CONCLUSIONS

Based on above discussion, the following can be listed as the conclusion.

1) The present study discussed about the flow field related to the boil phenomena. For this purpose, three different flow were compared, such as a) observed results by ADCP, b) observed results modified by the mass-consistent method, and c) numerically simulated results with URANS model.

2) The modification by the mass-consistent method does not change much for flow field on the line 1.

3) The vertical velocities were recognized at appropriate location, corelating with the shape of the bed form. However, observed velocity were smaller than that simulated by the URANS model.

4) The present study concluded that there are three significant characteristics of the boil, such as a) high upward velocity generates at the stoss side, b) longitudinal velocity is affected by the a), and c) the down-ward velocity generates at the top of the crest as a paired type flow with the a). The URANS model successfully simulated the boil phenomena in terms of a) and high Reynolds shear stress.

5) In addition to that, the present study discussed about the shear stress acting on the river bed by means of two different method, such as a) observed results by ADCP as bed load velocity, and b) numerically simulated results with URANS model.
6) Regarding 5), the both methods indicated the highest bed shear stress at the location of the boil, and it was about 1.05 times larger than the one at the top of the crest.

REFERENCES

Ali, M. S., Hosoda, T. and Kimura, I. (2007). A non-linear k-ε model to predict the spatial change of turbulent Structures in large scale vortices, *journal of Applied Mechanics*, JSCE, 10; 723-732.

Ashida, K. and Michiue, M. (1970). Study on the suspended sediment (1). Concentration of the suspended sediment near the bed surface. *Disaster Prevention Research Institute annuals*, 13B:233-242.

Egashira, S., Miyamoto, K., and Ito, T. (1997). Bed-load rate in view of two phase flow dynamics, *Proceedings of hydraulic engineering*, JSCE, 41:789-794.

Gul. A. A., Yorozuya, A., Koseki, H., Egashira, S., and Okada, S. (2018). Analysis of bedform and boil based on observations in Brahmaputra river, *Journal of Japan Society of Civil Engineers B1*, 74/5: 925-930.

Okada S., Yorozuya A., Koseki H., Kudo S., and Muraoka K.(2016). Comprehensive measurement techniques of water flow, bedload and suspended sediment in large river using Acoustic Doppler Current Profiler. *13th International Symposium on River Sedimentation, ISRS 2016*, At Stuttgart, Germany, pp 1274–1280.

Hashiba, M., Yorozuya, A., Koseki, H. (2017). Simulation of ADCP measurement in channel flows with multi-cellular secondary currents. *International Symposium and Exhibition on Hydro-Environment Sensors and Software*, pp.11-17.

Kimura, I. and Hosoda, T. (2000). Numerical analysis of flows around a cube by means of a non-linear k-ε model. *Proceedings of hydraulic engineering*, JSCE, 44:599-604.

Kinoshita, R. (1984). Present status and future prospects of river flow analysis by the aerial photograph, *Journal of Japan Society of Civil Engineers*, 345/II-1: 1-19.

Kitsuda, T., Arai, R., Minami, S., and Ryuu, H. (2004). Study about monitoring method of suspended sediment transport rate in actual river with ADCP, *Proceeding of forum in environmental engineering study*, 41: 22-24

Koseki, H., Yorozuya, A., Kudo, S., Kitsuda, T., and Iwami, Y. (2017). Evaluation of bed load discharge and effective friction velocity in rivers. *Journal of Japan Society of Civil Engineers B1*, 73/4: 763-768.

Nezu, I. and H. Nakagawa (1983). Turbulence in open-channel flows, A.A. Balkema Publishers, USA.

Nezu, I. and H. Nakagawa (1989). Accurate measurements of space-time correlations of coherent vortex behind dunes in turbulent open-channel flows with combination of laser-Doppler anemometer and hot-film anemometer. *Proc. Of instrumentation for hydraulic laboratories*, Canada centre for inland waters, pp.29-44.

Rennie, C.D., Millar, R. G., and Church, M. A. (2002). Measurement of bed load velocity using an Acoustic Doppler Current Profiler, *J. Hyd. Eng*. 128/5: 473-483.

Sekine, S. (2007). Study on dispersion process of suspended sediment on the basis of particle motion analysis, *Journal of Japan Society of Civil Engineers B*, 63/4: 311-322.

Sherman, C.A.(1978). A Mass-Consistent Model for Wind Fields over Complex Terrain. *J. Appl. Meteorol.* 17: 312-319

Yorozuya, A., Okada, S., Keizo, E., Kanno, Y., and Fukami, K. (2010), Method for estimating shear velocity and bedload discharge with Acoustic Doppler Current Profiler, *Annual journal of hydraulic engineering*, JSCE, 54:1093-1098.